PROCEEDINGS OF ECOS 2023 - THE 36TH INTERNATIONAL CONFERENCE ON
EFFICIENCY, **C**OST, **O**PTIMIZATION, **S**IMULATION AND ENVIRONMENTAL IMPACT OF ENERGY SYSTEMS
25-30 JUNE 2023, LAS PALMAS DE GRAN CANARIA, SPAIN

A Nonlinear Optimization Method for Expansion Planning of District Heating Systems with Graph Preprocessing

***Jerry Lambert*[a] *and Hartmut Spliethoff*[b]**

[a] *Technical University of Munich, Chair of Energy Systems Munich, Germany, jerry.lambert@tum.de, CA*
[b] *Technical University of Munich, Chair of Energy Systems Munich, Germany, spliethoff@tum.de*

Abstract:

This paper presents a method to find the optimal topology, pipe sizing, and operational parameters of a district heating system under consideration of one design point. The current high costs of district heating systems set limits regarding the minimum heat demand density required for economic network expansions. Optimized routing with ideal pipe sizing and optimal operating parameters offers a potential for cost reduction. With a lower network temperature, the consideration of nonlinear transport phenomena within the district heating network becomes increasingly important. Therefore, a new nonlinear optimization method is introduced, where graph preprocessing reduces the computational effort of the subsequent nonlinear optimization. A cost penalization method, using a smooth approximation of a Heaviside function is applied to pipe investment costs to account for discrete piping diameters. To guarantee fast convergence of the optimization algorithm, the Jacobian matrixes are calculated and the problem is solved with an interior point algorithm. As a proof of concept, the district heating system for a small fictional town with 42 consumers is optimized and analyzed. The whole nonlinear optimization is performed in 19.37 sec and in most cases discrete or near discrete diameters are achieved in a nonlinear continuous optimization.

Keywords:

Energy System, District Heating, Nonlinear Optimization, Topology Optimization.

1. Introduction

District heating systems can play a key role in a socially accepted, economic transformation towards a renewable energy system due to numerous advantages over a building-specific heat supply [1]. Currently, the high total costs of district heating systems usually require a high heat demand density for economic network expansions [2], as until recently there was very strong competition in the form of cheap individual heating from oil and gas. In addition, long amortization periods frequently prevent expansions from being economically feasible without subsidies. One possibility to reduce investment costs of district heating networks is a detailed nonlinear topology optimization, allowing optimized routing with ideal pipe sizing, as well as optimized operating parameters. Especially in less urbanized or rural areas, an untapped potential of environmentally friendly heat supply could be exploited [3]. In urban areas, [4] shows that an integration of industrial waste heat into district heating systems could further improve the potential of these systems. In the next section, different optimization techniques for district heating systems are explained in the following order: Mixed-integer linear programming (MILP), mixed-integer nonlinear programming (MINLP), heuristics, and adjoint-based optimization.

The discrete nature of network expansions and commercially available pipe diameters often leads to a mixed-integer programming formulation. [5] shows that most publications on district heating topology optimization are using MILP. In [6], mixed-integer linear programming is used to solve this structural optimization for a district cooling system. In [7], a similar MILP approach is used to perform a topology optimization of a single-commodity flow network. The optimization is reduced to a power flow in the network, neglecting e.g. mixing effects at junctions. Pressure dependencies are omitted. Different supply technologies, operational parameters and network topology are optimized in [8]. Heat losses are considered by calculating the enthalpy loss in a pipe with an average heat loss per unit length and pipe. Pressure losses in pipes were considered by linearizing the Haaland equation. Similar MILP formulations can be found in [9, 10]. In [11], a method is presented to create network topologies based on Geographic Information System data. In a second step, pressure losses are estimated in the network at the heat demand's peak load, and the pipe diameters are sized accordingly. [12] improved the method presented in [7] by calculating a maximal linear power flow with the help of a linearization based on a specific pressure loss and commercially available pipe diameters. [13] further improves on [12] by reducing the number of binary variables used in the optimization problem formulation. However, all these methods are not able to depict the nonlinear effects of district heating networks. Flow patterns in systems with

https://doi.org/10.52202/069564-0238

multiple spatial distributed producers, mixing temperatures at junctions or loops, can hardly be linearized while respecting the physical interrelations.

To combat these problems, mixed-integer nonlinear programming is used more frequently in recent publications. In [14], an MINLP is proposed to solve an operational-based optimal scheduling strategy to minimize the daily operational cost of an energy station with a heating and cooling demand, as well as storage. However, the distribution of the heat by a district heating network is neglected. The commercial MINLP solver DICOPT within GAMS is used in [15] to solve a nonlinear and discrete representation of a steady-state district heating system. In [16], the same method is used in a small-scale district heating system with 19 consumers. Moreover, the nonlinear effects of energy, as well as momentum conservation, are considered and solved with commercial solvers in [17, 18]. However, due to the nonlinear equations and the discrete nature of some variables, these methods are limited to a few consumers. [19] shows, solving the full MINLP leads to an exponential scaling of computational costs with network size during the discrete topology optimization.

Another method for solving district heating optimization problems is the use of heuristic optimization approaches. These procedures may provide a sufficiently good solution to an optimization problem while not always guaranteeing a local or global optimum. This becomes especially difficult with scaling dimensions of the problem. A commonly used heuristic approach are nature-inspired algorithms like the ant colony optimization or the genetic algorithm. In [20], the ant colony optimization was used to minimize fuel consumption while modelling a nonlinear gas flow. A parallel ant colony system algorithm is used in [21] to find a cost-optimal route between one producer and one consumer while neglecting the nonlinear effects of pressure or temperature dependencies, only considering investment costs of piping influenced by the surface condition. Similar in [22], the genetic algorithm is used to optimize a single long-distance heat transport system considering hydraulic and thermal nonlinear aspects. The genetic algorithm is used in [18] to optimize the district heating network topology and pipe diameters of a small network with ten heat consumers. Meanwhile, in [23], a hybrid strategy with a genetic algorithm and MILP is used to minimize the fuel costs of different heat producers. In [24], a methodology focusing on the optimal sizing of pipe diameters using a genetic algorithm to generate a set of Pareto-optimal sizing choices is presented.

The last presented optimization method is adjoint optimization. In [25], the adjoint method is used to optimize robust hydraulic district heating systems while neglecting thermal aspects within the network. Another adjoint method is presented in [26] that optimizes simultaneously the district heating topology and operational parameters of a district heating system. The method is further expanded in [27] and applied to a district of 160 consumers. The discrete optimization problem is transformed into a continuous optimization problem by using Heaviside functions. Moreover, constraint aggregation is used to increase the performance of the optimization procedure. In [28], the method of [27] is further developed by introducing a solid isotropic material with a penalization approach to reach discrete diameters.

2. Methodology

In this paper, the considered heat carrier medium is water at 60 °C. It is assumed to be liquid and therefore incompressible. Additionally, by assuming temperature changes smaller than $\Delta T = 40\,^{\circ}\mathrm{C}$, temperature dependencies of the fluid properties (e.g. density ρ, heat capacity c_p and dynamic viscosity μ) can be neglected. Moreover, this reduces the dependencies between the thermal and hydraulic parts of the optimization. During the nonlinear topology optimization of the district heating system, the following two main challenges occur:

- The formulation of equations in dependence of potential pipe connection (e.g. pressure or thermal losses in a pipe)
- The direction of the flow in pipes (e.g. mixing temperature in a node)

Therefore, a new preprocessing method is proposed to solve and improve the problems mentioned above. First, a linear thermal power flow optimization is performed on the district heating topology to determine flows through the network, eliminate unnecessary piping connections, and reduce the available choice of discrete piping diameters. Afterward, a detailed nonlinear optimization is performed on the preprocessed district heating system. In this optimization the nonlinear pressure and temperature drops as well as discrete diameters are determined, thus giving a far more realistic depiction of the network. First, in section 3. the graph representation of a district heating system is introduced. In section 4., the preprocessing method is explained, while the nonlinear optimization model is introduced in section 5.. Finally, in section 6. the results for a small district heating system of 42 consumers are shown and in section 7. a conclusion is drawn.

3. Representing a District Heating System as a Graph

To represent pipes, junctions, producers, or consumers mathematically a graph representation of a district heating system has to be introduced. The pipes of the district heating systems correspond to the arcs of the graph and the network's junctions to the nodes. The district heating network consists of a feed and return network which have arcs of opposite directions. This superstructure contains all possible connections and pathways from the heat source to the consumers. The set of all nodes N can be subdivided into three diffident subsets:

$$N_{int} \cup N_p \cup N_c = N \tag{1}$$

In Equation 1, *int* refers to all nodes without a consumer or a producer. The subscript p describes all nodes with a connection to at least one producer and the subscript c all nodes with a connection to at least one consumer. Similarly, A_{int} represents the geometrical pipe connection between two different internal nodes. A_p and A_c denote the state transition between the district heating system and a producer or a consumer. The set A representing all arcs of the network is given by:

$$A_{int} \cup A_p \cup A_c = A \tag{2}$$

A certain node of the network will be referred to as n, whereas a directed arc going from node i to node j as $ij \in A$.

4. Linear District Heating Model

In order to linearize the maximal power flow in a district heating pipe with length l, the maximal mass flow m with the corresponding velocities v of each considered piping diameter d has to be determined. First, the Bernoulli equation with a head loss Δh_f is used to calculate the pressure loss between two nodes i and j with equal height connected by a pipe:

$$\frac{p_i}{\rho} + \frac{v_i^2}{2} = \frac{p_j}{\rho} + \frac{v_j^2}{2} + \Delta h_f \tag{3}$$

The head loss Δh_f is calculated according to Darcy-Weisbach:

$$\Delta h_f = f_{ij} \cdot \frac{l_{ij}}{d_{ij}} \cdot \frac{v_{ij}^2}{2} \tag{4}$$

The Reynolds number Re is calculated as:

$$Re_{ij} = \frac{\rho \cdot v_{ij} \cdot d_{ij}}{\mu} \tag{5}$$

For Reynolds numbers $Re < 2320$ the friction factor f_{ij} is calculated by:

$$f_{ij} = \frac{64}{Re_{ij}} \tag{6}$$

The friction factor f_{ij} for $Re \geq 2320$ is given by the Haaland equation with the pipe roughness ε: [29]

$$f_{ij} = \left[-1.8 \cdot \log\left(\left(\frac{\varepsilon}{3.7 \cdot d_{ij}} \right)^{1.11} + \frac{6.9}{Re_{ij}} \right) \right]^{-2} \tag{7}$$

According to [30], the specific pressure drop per meter pipe length should range from 70 Pa/m to 350 Pa/m. In this study, a maximum specific pressure drop Δp_{max} of 250 Pa/m is assumed for the optimization. An iterative calculation is used to determine the maximal velocity in a pipe with a given inner diameter. Starting at an initial velocity of 0.01 m/s, the following equation is iterated until the relative difference of v between two consecutive steps is smaller than 10^{-6}:

$$v_{i+1} = \sqrt{\frac{2 \cdot \Delta p_{max} \cdot d}{f \cdot \rho}} \tag{8}$$

https://doi.org/10.52202/069564-0238

Finally, the maximal thermal power flow $\dot{Q}_{max}$ is calculated with the corresponding inner diameter and the feed and return line temperature. Next, the thermal aspect of an insulated pipe buried underground is considered. Therefore, the temperature difference Θ between the water temperature in the pipe T and the outside temperature T_∞ is introduced. In this study, T_∞ is set to 0 °C. The exit temperature Θ_{ij} of a pipe segment ij due to heat loss to its environment with an entry temperature Θ_i of the corresponding node is given by:

$$\Theta_{ij} = \Theta_i \cdot \exp\left(\frac{-l_{ij}}{c_p \cdot \dot{m}_{ij} \cdot R_{ij}}\right) \tag{9}$$

The combined thermal resistance of pipe and soil per unit length is calculated with the ratio r between outer and inner diameter: [27]

$$R_{ij} = \frac{\ln 4h/rd_{ij}}{2\pi\lambda_g} + \frac{\ln r}{2\pi\lambda_{insul}} \tag{10}$$

The ratio r in Equation 10 is determined with the actual inner diameter and the insulation thickness 1 based on [31]. After the hydraulic and thermal calculations, a linear regression of the investment costs and the thermal losses per trench length, using SciPy [32], is performed and shown in Figure 1. The total investment costs for piping are adapted from [2]. In this study, pipes ranging from DN20 to DN400 are considered.

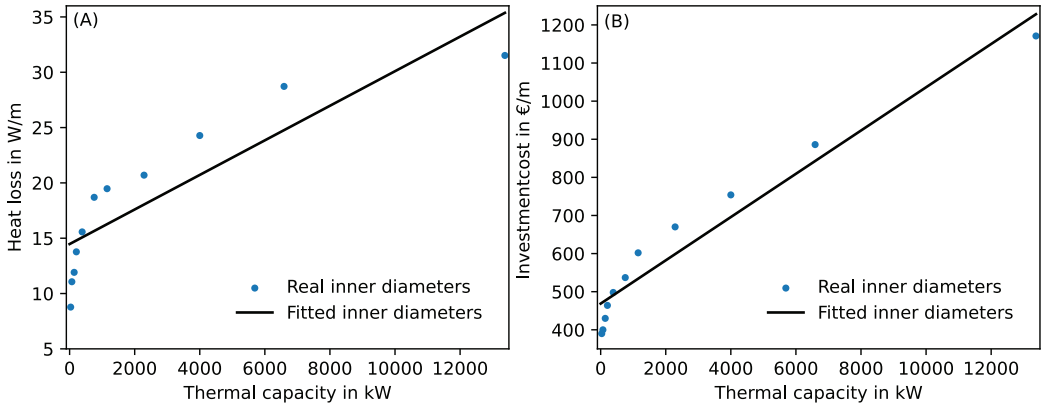

Figure 1: Optimization parameters of the district heating pipelines; (A) Thermal losses of the district heating pipes per trench length. (B) Costs of the district heating pipes per trench length.

.

Based on [7, 12], a mixed-integer linear programming model is introduced to calculate the optimal power flow through the district heating network, determine flow directions, and omit unnecessary connections. Therefore, a bi-directional pipe model is built. The thermal power input and output of every pipe are modelled according to the directed graph of the network. In order to allow flows in the opposite direction, every potential pipe ij is also modelled in the direction ji. The use of a pipe in a unique direction is assured by the objective function (see Equation 16). For simplicity, only the equations for pipes in the direction ij are provided. The heat outflow $\dot{Q}_{out}$ of each pipe results from the inflow $\dot{Q}_{in}$ minus the thermal loss $\dot{Q}_{loss}$:

$$\dot{Q}_{ij,in} - \dot{Q}_{ij,out} - \dot{Q}_{ij,loss} = 0 \tag{11}$$

$$\dot{Q}_{ij,in} \leq \dot{Q}_{max,cons} \cdot \lambda_{ij} \tag{12}$$

$$\dot{Q}_{ij,in} \leq \dot{Q}_{max} \tag{13}$$

In Equation 12, the binary variable λ_{ij} shows the usage of a potential pipe. Moreover, $\dot{Q}_{max,cons}$ can be seen as a Big-M-constraint, enforcing zero thermal flow if the direction ij of the pipe is not used. Meanwhile, in

Equation 13 the actual maximal thermal capacity $\dot{Q}_{max}$ is determined. This value is independent of the flow direction (*ij* or *ji*). The thermal losses are determined by the linear regression factor a_{therm} and b_{therm}:

$$\dot{Q}_{ij,loss} = \left(a_{therm} \cdot \dot{Q}_{ij,in} + b_{therm} \cdot \lambda ij\right) \cdot l_{ij} \tag{14}$$

Each connection of a consumer to the district heating grid is modelled unidirectional, and thus no heat feed-in from a consumer is possible. Moreover, energy conservation is assumed in every node under consideration of the consumer's heat demand and the heat source's feed-in:

$$\sum_{ij \in A_i} \dot{Q}_{ij} - \sum_{ji \in A_i} \dot{Q}_{ji} - \sum_{c \in A_c} \dot{Q}_c + \sum_{p \in A_p} \dot{Q}_p = 0 \tag{15}$$

Finally, the objective function aims to minimize the total investment costs of the district heating network under a set of given consumers which need to be connected to the grid. As every consumer's connection to the grid is mandatory, the investment costs in the objective function are not distributed over the depreciation period and no operational costs are considered. The investment costs are determined by the linear regression factors a_{cost} and b_{cost} from Figure 1:

$$min\left\{ \sum_{A_i} \left(a_{cost} \cdot \dot{Q}_{max} + b_{cost} \cdot (\lambda_{ij} + \lambda_{ji})\right) \cdot l_{ij} \right\} \tag{16}$$

The corresponding pipe diameter to the maximal heat flow $\dot{Q}_{max}$ can be calculated with fsolve from [32] with Equation 8. The initially assumed flow direction in the graph can be corrected according to λ_{ij} and λ_{ji}:

- $\lambda_{ij} = 0$ and $\lambda_{ji} = 0$: The pipe is not used and can be deleted from the graph.
- $\lambda_{ij} = 1$ and $\lambda_{ji} = 0$: The assumed flow direction in the graph is correct.
- $\lambda_{ij} = 0$ and $\lambda_{ji} = 1$: The flow direction in the graph is the opposite of the assumed one and needs to be corrected.

The linear diameter *d* and the corrected graph can be used to facilitate and speed up the nonlinear topology optimization, described in section 5.. Here, based on the linear diameter, determined by the preprocessing method, the choice of the available diameter is limited to the next and the following larger one.

5. Nonlinear District Heating Model

To account for more complex influences, such as mixing temperatures or pressure drops, a nonlinear transport model has to be developed. First, a nonlinear model for district heating pipes is presented. Subsequently, nonlinear models for consumers and heat sources are introduced. Finally, the objective functions and the pipe discretization method used are shown.

5.1. Transport Model

Similar to section 4., the pressure loss through any given pipe in the network has to be determined. By using the Haaland equation (see Equation 7) during the pressure loss calculations, the flow in the pipes is assumed to be turbulent. This flow regime is desired in a district heating network, to ensure a well-defined and continuous flow through the pipes. When Equation 3-5 are combined and the velocities converted to mass flows ($m_{ij} = (v_{ij} \cdot \pi \cdot d_{ij}^2)/(4 \cdot \rho)$), the pressure loss can be calculated as:

$$p_i - p_j = \frac{8 \cdot f_{ij}}{\pi^2 \cdot \rho} \cdot \frac{l_{ij}}{d_{ij}^5} \cdot \dot{m}_{ij}^2 \tag{17}$$

Analogical to section 4., a maximal specific pressure drop Δp_{max} in a pipe *ij* is imposed:

$$p_i - p_j \leq l_{ij} \cdot \Delta p_{max} \tag{18}$$

In each node *i* mass conservation must be fulfilled:

$$\sum_{ij \in A_i} \dot{m}_{ij} - \sum_{ji \in A_i} \dot{m}_{ji} - \sum_{c \in A_c} \dot{m}_c + \sum_{p \in A_p} \dot{m}_p = 0 \tag{19}$$

https://doi.org/10.52202/069564-0238

Moreover, inside a node of the district heating system, perfect mixing of the incoming fluids is assumed. All outgoing flows depart from the node with the corresponding node temperature Θ_n and energy is conserved in every node of the system:

$$\sum_{in \in A} \left(\dot{m}_{in} \cdot \Theta_{ij} \right) - \sum_{nj \in A} \left(\dot{m}_{nj} \cdot \Theta_n \right) = 0 \tag{20}$$

Heat losses are calculated analogously to section 4.. Only in Equation 10 a fixed ratio $d_{o,ij} = r \cdot d_{ij}$ between the outer and inner diameter of a pipe is assumed. In this study, r is set to 4.

5.2. Producer Model

At the producer, a fixed exit temperature of 90 °C is imposed as a boundary condition for the district heating system. In addition, a reference pressure is defined in one of the producer's return nodes to define the pressure throughout the network. As only pressure differences influence the mass flow solution, the solution is independent of the chosen reference. In Equation 21-22 *flh* refers to full load hours of the district heating network. In this study, the district heating network is assumed to have 2500 full load hours [33]. To consider pumping costs C_{pump} during the optimization, the electric power consumption of the pump is modelled with a constant efficiency η_{pump} and the specific electric power costs c_{el}:

$$C_{pump} = \frac{\dot{m}_p}{\rho} \cdot \frac{1}{\eta_{pump}} \cdot (p_i - p_j) \cdot flh \cdot c_{el} \tag{21}$$

Moreover, the optimization has to be able to benchmark different heat producers against each other. Therefore, the fuel costs C_{fuel} at each producer with the specific fuel costs c_{fuel} are considered:

$$C_{fuel} = \dot{m}_p \cdot c_{p,water} \cdot (\Theta_p - \Theta_i) \cdot flh \cdot c_{fuel} \tag{22}$$

5.3. Consumer Model

In the nonlinear optimization, every consumer is modelled with an individual substation. Each substation is composed of a heat exchanger and a throttle. This throttling configuration, shown in Figure 2, allows a variable mass flow in the district heating's and the consumer's circuit to control the heat transferred to the consumer, as well as low return flow temperatures with low flow velocities during partial load [31].

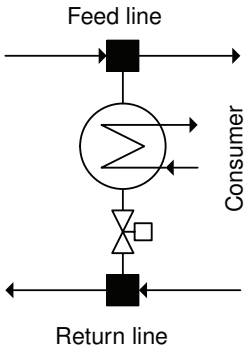

Figure 2: Configuration of a consumer substation in the district heating system.

The pressure drop over a consumer c which connects node f in the feed line and node r in the return line is assumed to be of the following form:

$$p_f - p_r - p_{throttle} = \Delta p_{des} \tag{23}$$

In this study, the design pressure drop Δp_{des} over each substation is set to 0.5 bar. To increase the numerical stability of the optimization, the heat demand of every consumer connected to the grid must be satisfied within a range of 95 % to 110 %:

$$0.95 \cdot \dot{Q}_c \leq c_{p,water} \cdot \dot{m}_c \cdot (\Theta_f - \Theta_c) \leq 1.10 \cdot \dot{Q}_c \tag{24}$$

Here, the minimal cooling temperature Θ_c at the exit of each substation is set to 55 °C.

https://doi.org/10.52202/069564-0238

5.4. Pipe Discretization

Thus far, the presented algorithm still allows continuous diameters. In order to perform a more realistic topology optimization, the algorithm should be able to do discrete choices in a continuous optimization. Therefore, based on [27], a numerical continuation strategy that gradually forces the continuous diameter variables into discrete diameter choices is introduced. A smoothed projection of the diameters onto the discrete diameter set is gradually enforced and intermediate diameters are more and more penalized through the piping cost relation (see subsection 5.5.). For the projection of the diameters on the discrete diameter set, a smooth approximation of a Heaviside function is used: [27]

$$P(x,\sigma,\chi) = \frac{tanh(\chi\cdot\sigma) + tanh(\chi\cdot(x-\sigma))}{tanh(\chi\cdot\sigma) + tanh(\chi\cdot(1-\sigma))} \tag{25}$$

In Equation 25 the continuous decision variable $x \in [0,1]$ is gradually projected onto a binary decision variable $\tilde{x} \in \{0,1\}$. The variable $\chi \in]0,\infty[$ controls the steepness of the Heaviside approximation, while $\sigma \in [0,1]$ determines the threshold above which the variable x is projected onto the upper limit [27]. To account for the gradient-based optimization and to improve the stability of the optimization, the projection P is interpolated with a linear function, controlled by the factor ν: [27]

$$-10^{-3} \leq \nu\cdot\left(d_1 + (d_2-d_1)\cdot P\left(\frac{d-d_1}{d_2-d_1}, 0.01, \chi\right)\right) + (1-\nu)\cdot d \leq 10^{-3} \tag{26}$$

In Figure 3 different parameterizations for χ and ν of Equation 26 are shown with $d_1 = 0.1603\,\text{m}$ and $d_2 = 0.2101\,\text{m}$.

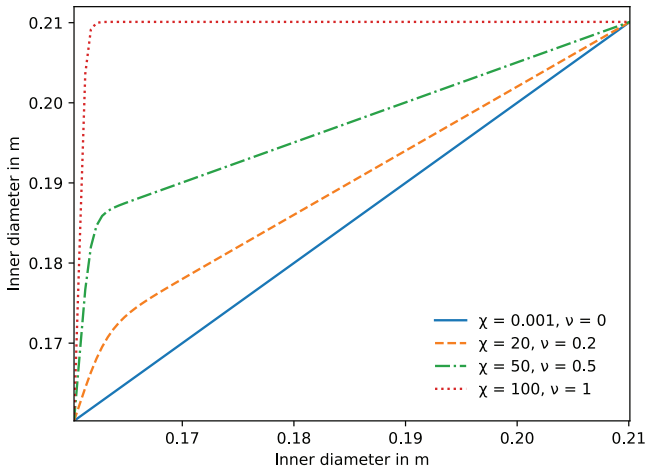

Figure 3: Function for pipe discretization for different values of χ and ν with $d_1 = 0.1603\,\text{m}$ and $d_2 = 0.2101\,\text{m}$

.

5.5. Objective Function

Similar to the pipe discretization method, the smooth approximation of a Heaviside function (see Equation 25) is used to penalize intermediate piping diameters during the optimization. To improve stability and to account for the gradient-based optimization, the projection is also interpolated with a linear function, controlled by the parameter ν. The investment costs for district heating pipes in the feed and return line C_{pipe}, connecting node i and j, are given by:

$$C_{pipe} = \left[\nu\cdot\left(c_1 + (c_2-c_1)\cdot P\left(\frac{d-d_1}{d_2-d_1}, 0.5, \chi\right)\right) + (1-\nu)\cdot\left(c_1 + (c_2-c_1)\cdot\frac{d-d_1}{d_2-d_1}\right)\right]\cdot l_{ij}\cdot 2\cdot A \tag{27}$$

In Equation 27, investment costs are distributed over the depreciation period n, using the annuity method. Without discounting, the annuity A is calculated with an interest rate i:

$$A = \frac{(1+i)^n\cdot i}{(1+i)^n - 1} \tag{28}$$

https://doi.org/10.52202/069564-0238

After [34], the depreciation period is set to 20 years and the interest rate i to 0.08. The objective function is formed by combining Equation 21, 22, and 27 and thus minimizing investment and operational costs. In Figure 4, different parameterizations of χ and ν for the investment costs of pipes are shown.

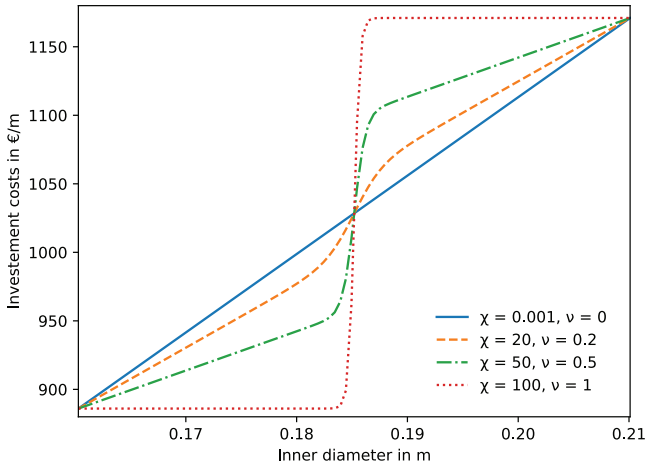

Figure 4: Heavyside projection of pipe investment cost for $d_1 = 0.1603\,\text{m}$ and $d_2 = 0.2101\,\text{m}$ with different values of χ and ν.

6. Example

The linear optimization is solved with Cplex 12.10.0 [35] using Pyomo [36, 37]. The nonlinear optimization is formulated with pyoptsparse [38] and solved with the interior point optimizer Ipopt [39]. An exemplary district heating system with 42 consumers is used to demonstrate the presented method. As every connection of a consumer to the grid is mandatory, independent of its economic efficiency, the preprocessing algorithm can only find the most favorable pathway to connect all consumers and delete dispensable pipes in the graph. The original network consists of 72 pipes. After the linear optimization, this is reduced to 69 pipes and 5 flow directions have been corrected, as shown in Figure 5. Here, the orange point represents the producer, grey nodes junctions, and blue nodes consumer in the district heating system. During preprocessing, the linear diameters, with their corresponding mass flows are determined and handed to the nonlinear optimization to be discretized. Due to the formulation of Equation 26, slight deviations from discrete diameters are allowed, but occur only in rare cases, as shown in Figure 6.

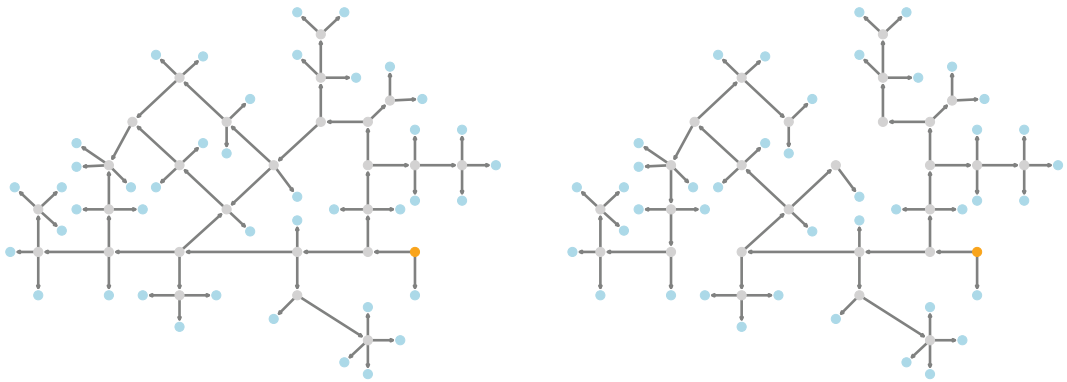

(a) Original (b) Preprocessed

Figure 5: Representation of the original and preprocessed network.

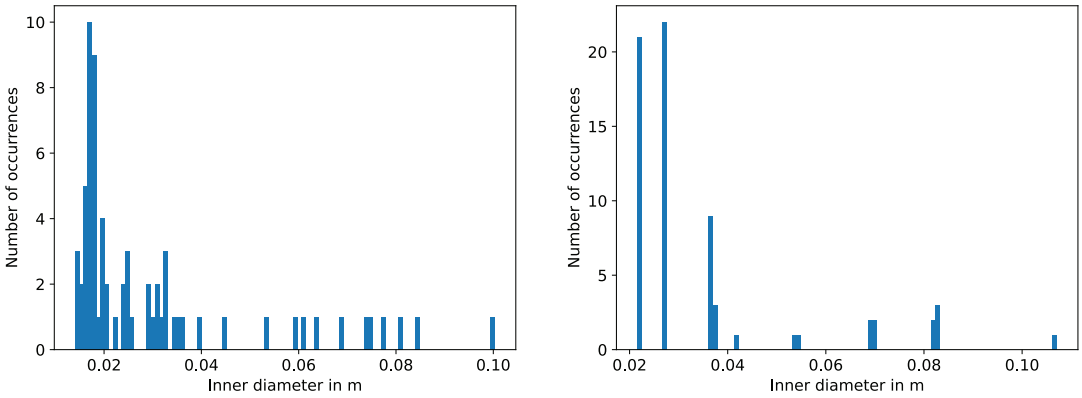

(a) Linear diameters (b) Discrete diameters

Figure 6: Distribution of the inner diameters before and after the nonlinear optimization with 100 bins between DN20 and DN200.

The nonlinear optimization is iteratively performed while increasing in each iteration the value of ξ and ν. Over ten iterations, ξ is evenly spaced out from 0.001 to 100 and ν from 0 to 1. The whole nonlinear optimization is performed in 19.37 sec. Linear diameters below DN20 are assigned either to DN20 or DN25, as shown in Figure 6. For some connections to smaller consumers, DN25 is oversized, as the optimizer tries to find a viable solution under consideration of all thermohydraulic equations and Equation 26. If an oversized solution, respecting the constraints is found, it can be difficult for the optimizer to revert to the smaller diameter, as the differences in operational and investment costs for two subsequent diameters are rather small. The resulting pressure profile of the district heating network can be seen in Figure 7. The highest cumulative pressure losses can be observed at the most remote consumer, defining the pressure level at the heat source. By comparing Figure 7a and 7b, a maximal pressure difference, larger than the assumed constant pressure drop over a consumer's substation, can be seen. In the modelled throttle, a pressure offset occurs between the feed and the return network, which raises the pressure level in the feed network artificially. As the pressure level does not affect the sizing of the pipes but only the pressure differences and as the pumping costs are rather small compared to the investment costs of the district heating system, this offset is not reduced during the optimization.

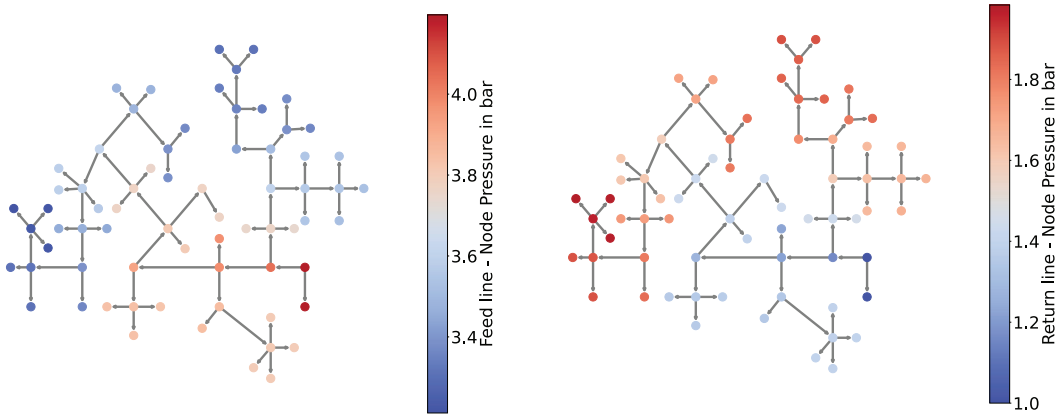

(a) Feed network (b) Return network

Figure 7: Resulting pressure profile in the feed and return network.

Figure 8 shows the resulting temperature profile after the nonlinear optimization. As shown in Figure 8b the consumer always tries to maximize the energy available to them in order to satisfy their demands and are

https://doi.org/10.52202/069564-0238

cooling the fluid down to 55 °C. The desired heat demand is met with 95 % of the desired heat, thus minimizing the operational costs. Overall a total efficiency for the heat distribution of 98.01 % is reached.

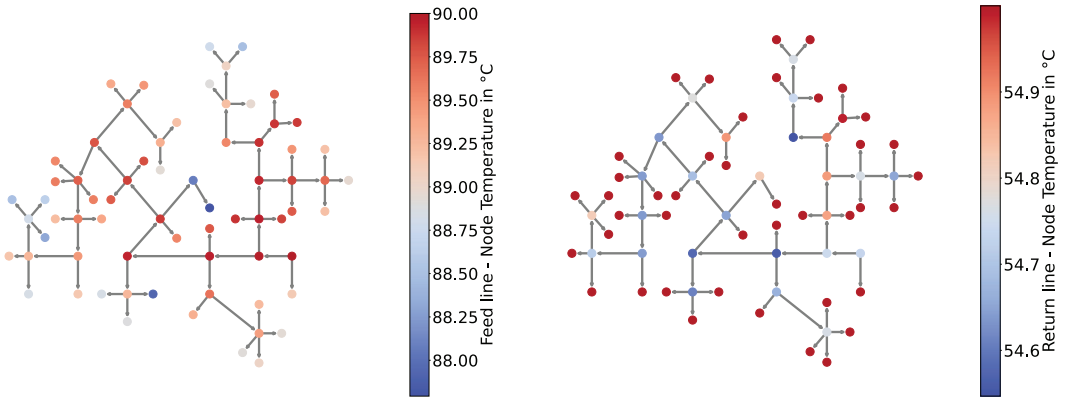

(a) Feed Network (b) Return Network

Figure 8: Resulting temperature profile in the feed and return network.

7. Conclusion and Outlook

A two-step methodology for the optimization of a district heating network, based on a thermohydraulic model, is derived and successfully implemented as an optimization problem. This method allows a fast nonlinear optimization of a district heating system. The method presented in this paper allowed the optimization of a small exemplary district heating system. Given a set of possible pipeline configurations to connect all the consumers to the grid regardless of its economic viability, the simulation was able to derive an optimal network design. The determined network configuration aimed at minimization of investment and operational costs.

In further works, the method should be applied to larger districts to prove the scalability of the method. Moreover, the discrete pipe sizing method should be improved to eliminate all non-discrete diameters in the final results of the optimization. The optimization should also be developed to account for the profitability of the considered district heating network. Therefore, the preprocessing method could be extended to determine the profitability of a potential connection of a consumer to the grid. Moreover, the nonlinear depiction of the district heating grid could be further improved. In this study, a constant ratio between inner and outer diameter is assumed. In real pipes, this ratio decreases with increasing inner diameter. Gradient-based nonlinear optimization converges always into a local optimum, a global optimum is not guaranteed. Therefore, it should be investigated how different possible local minima can be compared to one another and how the optimization can efficiently choose between the different local minima that occurred during the optimization. At last, the influence of the preprocessing method on the final results should be investigated.

Funding

This work was supported by the ”Bayerische Forschungsstiftung” in the framework of the project ”Sektorkopplung und Microgrids” (STROM) [project no.: AZ-1473-20]. The financial support is gratefully acknowledged.

References

[1] S. Werner, “International review of district heating and cooling,” *Energy*, vol. 137, pp. 617–631, 2017. doi: 10.1016/j.energy.2017.04.045

[2] T. Nussbaumer and S. Thalmann, “Influence of system design on heat distribution costs in district heating,” *Energy*, vol. 101, pp. 496–505, 2016. doi: 10.1016/j.energy.2016.02.062

[3] A. Jentsch, K. Bohn, A. Pohlig, C. Dötsch, S. Richter, and M. Manderfeld, “Handbuch zur Entscheidungsunterstützung. Fernwärme in der Fläche: Leitungsgebundene Wärmeversorgung im ländlichen Raum.”

[4] U. Persson, B. Möller, and S. Werner, “Heat Roadmap Europe: Identifying strategic heat synergy regions,” *Energy Policy*, vol. 74, pp. 663–681, 2014. doi: 10.1016/j.enpol.2014.07.015

[5] M. Sporleder, M. Rath, and M. Ragwitz, “Design optimization of district heating systems: A review,” *Frontiers in Energy Research*, vol. 10, 2022. doi: 10.3389/fenrg.2022.971912

[6] J. Söderman, “Optimisation of structure and operation of district cooling networks in urban regions,” *Applied Thermal Engineering*, vol. 27, no. 16, pp. 2665–2676, 2007. doi: 10.1016/j.applthermaleng.2007.05.004

[7] J. Dorfner and T. Hamacher, “Large-Scale District Heating Network Optimization,” *IEEE Transactions on Smart Grid*, vol. 5, no. 4, pp. 1884–1891, 2014. doi: 10.1109/TSG.2013.2295856

[8] C. Haikarainen, F. Pettersson, and H. Saxén, “A model for structural and operational optimization of distributed energy systems,” *Applied Thermal Engineering*, vol. 70, no. 1, pp. 211–218, 2014. doi: 10.1016/j.applthermaleng.2014.04.049

[9] B. Morvaj, R. Evins, and J. Carmeliet, “Optimising urban energy systems: Simultaneous system sizing, operation and district heating network layout,” *Energy*, vol. 116, pp. 619–636, 2016. doi: 10.1016/j.energy.2016.09.139

[10] C. Bordin, A. Gordini, and D. Vigo, “An optimization approach for district heating strategic network design,” *European Journal of Operational Research*, vol. 252, no. 1, pp. 296–307, 2016. doi: 10.1016/j.ejor.2015.12.049

[11] Marcus Fuchs and Dirk Müller, “Automated Design and Model Generation for a District Heating Network from OpenStreetMap Data,” 2017.

[12] T. Résimont, Q. Louveaux, and P. Dewallef, “Optimization Tool for the Strategic Outline and Sizing of District Heating Networks Using a Geographic Information System,” *Energies*, vol. 14, no. 17, p. 5575, 2021. doi: 10.3390/en14175575

[13] J. Röder, B. Meyer, U. Krien, J. Zimmermann, T. Stührmann, and E. Zondervan, “Optimal Design of District Heating Networks with Distributed Thermal Energy Storages – Method and Case Study: 5-22 Pages / International Journal of Sustainable Energy Planning and Management, Vol. 31 (2021),” 2021. doi: 10.5278/IJSEPM.6248

[14] N. Deng, R. Cai, Y. Gao, Z. Zhou, G. He, D. Liu, and A. Zhang, “A MINLP model of optimal scheduling for a district heating and cooling system: A case study of an energy station in Tianjin,” *Energy*, vol. 141, pp. 1750–1763, 2017. doi: 10.1016/j.energy.2017.10.130

[15] T. Mertz, S. Serra, A. Henon, and J.-M. Reneaume, “A MINLP optimization of the configuration and the design of a district heating network: Academic study cases,” *Energy*, vol. 117, pp. 450–464, 2016. doi: 10.1016/j.energy.2016.07.106

[16] T. Mertz, S. Serra, A. Henon, and J. M. Reneaume, “A MINLP optimization of the configuration and the design of a district heating network: study case on an existing site,” *Energy Procedia*, vol. 116, pp. 236–248, 2017. doi: 10.1016/j.egypro.2017.05.071

[17] F. Marty, S. Serra, S. Sochard, and J.-M. Reneaume, “Simultaneous optimization of the district heating network topology and the Organic Rankine Cycle sizing of a geothermal plant,” *Energy*, vol. 159, pp. 1060–1074, 2018. doi: 10.1016/j.energy.2018.05.110

[18] H. Li and S. Svendsen, “District Heating Network Design and Configuration Optimization with Genetic Algorithm,” *Journal of Sustainable Development of Energy, Water and Environment Systems*, vol. 1, no. 4, pp. 291–303, 2013. doi: 10.13044/j.sdewes.2013.01.0022

[19] Y. Wack, S. Serra, M. Baelmans, J.-M. Reneaume, and M. Blommaert, “Non-linear Topology Optimization of District Heating Networks: A benchmark of Mixed-Integer and Adjoint Approaches.” [Online]. Available: http://arxiv.org/pdf/2302.14555v1

[20] A. Chebouba, F. Yalaoui, L. Amodeo, A. Smati, and A. Tairi, “New Method to Minimize Fuel Consumption of Gas Pipeline Using Ant Colony Optimization Algorithms,” in *2006 International Conference on Service Systems and Service Management*. IEEE, 10/25/2006 - 10/27/2006. doi: 10.1109/ICSSSM.2006.320759. ISBN 1-4244-0451-7 pp. 947–952.

[21] Y. Zhang, G. Zhang, H. Zhao, Y. Cao, Q. Liu, Z. Shen, and A. Li, “A Convenient Tool for District Heating Route Optimization Based on Parallel Ant Colony System Algorithm and 3D WebGIS,” *ISPRS International Journal of Geo-Information*, vol. 8, no. 5, p. 225, 2019. doi: 10.3390/ijgi8050225

 https://doi.org/10.52202/069564-0238

[22] P. Hirsch, M. Grochowski, and K. Duzinkiewicz, “Decision support system for design of long distance heat transportation system,” *Energy and Buildings*, vol. 173, pp. 378–388, 2018. doi: 10.1016/j.enbuild.2018.05.010

[23] M. Vesterlund, A. Toffolo, and J. Dahl, “Optimization of multi-source complex district heating network, a case study,” *Energy*, vol. 126, pp. 53–63, 2017. doi: 10.1016/j.energy.2017.03.018

[24] Y. Merlet, R. Baviere, and N. Vasset, “Formulation and assessment of multi-objective optimal sizing of district heating network,” *Energy*, vol. 252, p. 123997, 2022. doi: 10.1016/j.energy.2022.123997

[25] A. Pizzolato, A. Sciacovelli, and V. Verda, “Topology Optimization of Robust District Heating Networks,” *Journal of Energy Resources Technology*, vol. 140, no. 2, 2018. doi: 10.1115/1.4038312

[26] M. Blommaert, R. Salenbien, and M. Baelmans, “AN ADJOINT APPROACH TO THERMAL NETWORK TOPOLOGY OPTIMIZATION,” in *International Heat Transfer Conference 16*. Connecticut: Begellhouse, 8/10/2018 - 8/15/2018. doi: 10.1615/IHTC16.cms.024074 pp. 2081–2089.

[27] M. Blommaert, Y. Wack, and M. Baelmans, “An adjoint optimization approach for the topological design of large-scale district heating networks based on nonlinear models,” *Applied Energy*, vol. 280, p. 116025, 2020. doi: 10.1016/j.apenergy.2020.116025

[28] Y. Wack, M. Baelmans, R. Salenbien, and M. Blommaert, “Economic Topology Optimization of District Heating Networks using a Pipe Penalization Approach,” *Energy*, vol. 264, no. 1, p. 126161, 2023. doi: 10.1016/j.energy.2022.126161. [Online]. Available: http://arxiv.org/pdf/2205.12019v2

[29] S. E. Haaland, “Simple and Explicit Formulas for the Friction Factor in Turbulent Pipe Flow,” *Journal of Fluids Engineering*, vol. 105, no. 1, pp. 89–90, 1983. doi: 10.1115/1.3240948

[30] I. Best, J. Orozaliev, and K. Vajen, “Impact of Different Design Guidelines on the Total Distribution Costs of 4th Generation District Heating Networks,” *Energy Procedia*, vol. 149, pp. 151–160, 2018. doi: 10.1016/j.egypro.2018.08.179

[31] *Planungshandbuch Fernwärme*, Version 1.1 vom 21. september 2017 ed. Ittigen and Bern: EnergieSchweiz Bundesamt für Energie, 21. September 2017. ISBN 3-908705-30-4

[32] P. Virtanen, R. Gommers, T. E. Oliphant, M. Haberland, T. Reddy, D. Cournapeau, E. Burovski, P. Peterson, W. Weckesser, J. Bright, S. J. van der Walt, M. Brett, J. Wilson, K. J. Millman, N. Mayorov, A. R. J. Nelson, E. Jones, R. Kern, E. Larson, C. J. Carey, Polat, VanderPlas, Jake, D. Laxalde, J. Perktold, R. Cimrman, I. Henriksen, E. A. Quintero, C. R. Harris, A. M. Archibald, A. H. Ribeiro, F. Pedregosa, P. van Mulbregt, and SciPy 1.0 Contributors, “SciPy 1.0: Fundamental Algorithms for Scientific Computing in Python,” *Nature Methods*, vol. 17, pp. 261–272, 2020. doi: 10.1038/s41592-019-0686-2

[33] European Commission. Directorate General for Energy., TU Wien., Tilia GmbH., Institute for Resource Efficiency and Energy Strategies GmbH., Fraunhofer ISI., and Öko Institut., *District heating and cooling in the European Union: overview of markets and regulatory frameworks under the revised Renewable Energy Directive*. Publications Office, 2022.

[34] AGFW, “FW 704 - Wirtschaftlichkeit nach §§ 20 und 24 KWKG - Pauschalierte Kennwerte,” 07.03.2023. [Online]. Available: https://www.fw704.de/hauptmenue/kennwerte/pauschalierte-kennwerte

[35] Cplex, “ILOG CPLEX Optimization Studio,” 2023. [Online]. Available: https://www.ibm.com/de-de/products/ilog-cplex-optimization-studio

[36] M. L. Bynum, G. A. Hackebeil, W. E. Hart, C. D. Laird, B. L. Nicholson, J. D. Siirola, J.-P. Watson, and D. L. Woodruff, *Pyomo — Optimization Modeling in Python*, 3rd ed., ser. Springer eBook Collection. Cham: Springer International Publishing and Imprint Springer, 2021, vol. 67. ISBN 9783030689285

[37] W. E. Hart, J.-P. Watson, and D. L. Woodruff, “Pyomo: modeling and solving mathematical programs in Python,” *Mathematical Programming Computation*, vol. 3, no. 3, pp. 219–260, 2011. doi: 10.1007/s12532-011-0026-8

[38] N. Wu, G. Kenway, C. Mader, J. Jasa, and J. Martins, “pyOptSparse: A Python framework for large-scale constrained nonlinear optimization of sparse systems,” *Journal of Open Source Software*, vol. 5, no. 54, p. 2564, 2020. doi: 10.21105/joss.02564

[39] A. Wächter and L. T. Biegler, “On the implementation of an interior-point filter line-search algorithm for large-scale nonlinear programming,” *Mathematical Programming*, vol. 106, no. 1, pp. 25–57, 2006. doi: 10.1007/s10107-004-0559-y